LIBRARY OF THE
UNIVERSITY OF ILLINOIS
AT URBANA-CHAMPAIGN

510.84
Il6r
no.171-187
cop.2

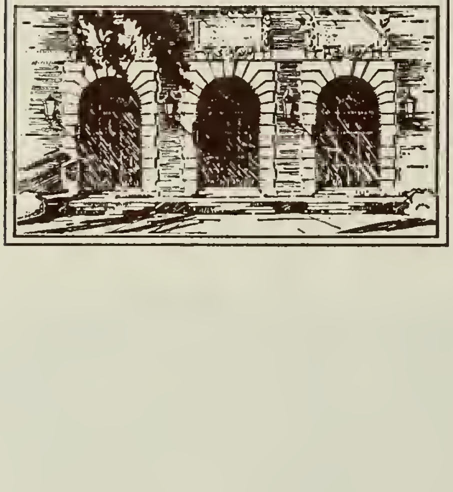

Digitized by the Internet Archive
in 2013

http://archive.org/details/pathintegralcalc186fosd

l6r
186
cop 3

Report No. 186

PATH INTEGRAL CALCULATION OF THE TWO-PARTICLE SLATER SUM FOR He_4

by

Lloyd D. Fosdick
Harry F. Jordan

UNIVERSITY OF ILLINOIS
AUG 19 1966
LIBRARY

August 20, 1965

DEPARTMENT OF COMPUTER SCIENCE · UNIVERSITY OF ILLINOIS · URBANA, ILLINOIS

Report No. 186

PATH INTEGRAL CALCULATION OF THE TWO-PARTICLE SLATER SUM FOR He_4

by

Lloyd D. Fosdick
Harry F. Jordan

August 20, 1965

Department of Computer Science
University of Illinois
Urbana, Illinois

Path Integral Calculation of the Two-Particle Slater Sum for He_4[†]

Lloyd D. Fosdick and Harry F. Jordan
Department of Computer Science and Department of Physics
University of Illinois, Urbana, Illinois

ABSTRACT

The Wiener integral formulation combined with Monte Carlo sampling has been used to compute the two-particle Slater sum for He_4 for temperatures ranging from 273° K down to 2° K, the lower practical limit for this computational method. This is equivalent to a calculation of the density independent part of the pair distribution function. A Lennard-Jones 6-12 potential has been used to describe the interaction. Contributions from exchange were found negligible at 5° K and above. Comparisons with the Wigner-Kirkwood expansion are made. The second virial coefficients derived from these results are within two per cent or three per cent of the results obtained from the usual phase shift calculation.

1. INTRODUCTION

For a system of N identical particles of mass m enclosed in a volume Ω, with Hamiltonian H_N, the Slater sum[1] is

$$W_N = N!\, \lambda^{3N} \sum_i \Psi_i^* (\underset{\sim}{1}, \underset{\sim}{2}, \ldots, \underset{\sim}{N}) e^{-\beta H_N} \Psi_i(\underset{\sim}{1}, \underset{\sim}{2}, \ldots, \underset{\sim}{N}), \tag{1.1}$$

where $\Psi_i(\underset{\sim}{1}, \ldots, \underset{\sim}{N})$ is the wave function of the system in the state i; $\underset{\sim}{1}$ is the position coordinate of particle 1, $\underset{\sim}{2}$ is the position coordinate of particle 2, etc.; λ is the thermal wave length

$$\lambda = \left(\frac{2\pi\hbar^2\beta}{m}\right)^{\frac{1}{2}}; \tag{1.2}$$

and

$$\beta = \frac{1}{kT}. \tag{1.3}$$

The wave functions are normalized to 1 in the volume Ω,

$$\int_\Omega \Psi_i^* (\underset{\sim}{1}, \underset{\sim}{2}, \ldots, \underset{\sim}{N}) \Psi_i(\underset{\sim}{1}, \underset{\sim}{2}, \ldots, \underset{\sim}{N}) d^3\underset{\sim}{1} d^3\underset{\sim}{2} \ldots d^3\underset{\sim}{N} = 1, \tag{1.4}$$

and the summation in Eq. (1.1) extends over all states appropriate to the statistics of the system. A superscript is used on W_N to explicitly denote Bose-Einstein (W_N^B) or Fermi-Dirac (W_N^F) statistics.

We present here the results of computing W_2^B for ten temperatures extending from 273° K down to 2° K. The potential describing the interaction is the Lennard-Jones 6-12 potential

$$V = 4\alpha\left((\frac{\sigma}{r})^{12} - (\frac{\sigma}{r})^{6} \right), \tag{1.5}$$

where α and σ are the deBoer, Michels[2] values appropriate to He_4:

$$\begin{aligned} \alpha &= 14.04 \times 10^{-16} \text{ erg}, \\ \sigma &= 2.56 \times 10^{-8} \text{ cm}. \end{aligned} \tag{1.6}$$

A central feature of this calculation is the use of the Wiener integral formulation of the Slater sum,[3] described in the following section. The Wiener integrals have been evaluated by a Monte Carlo sampling scheme on the ILLIAC II computer.

The results exhibited here are appropriate to a description of the pair distribution function $n_2(\underset{\sim}{1}, \underset{\sim}{2})$ at very low densities. This function is given by

$$n_2(\underset{\sim}{1}, \underset{\sim}{2}) = \frac{1}{(N-2)!\lambda^{3N} Q_N} \int_{\Omega} W_N(\underset{\sim}{1}, \underset{\sim}{2}, \ldots, \underset{\sim}{N}) d^3\underset{\sim}{3}, d^3\underset{\sim}{4}, \ldots, d^3\underset{\sim}{N}, \tag{1.7}$$

where Q_N is the partition function

$$Q_N(T,\Omega) = \frac{1}{N!\lambda^{3N}} \int_{\Omega} W_N(\underset{\sim}{1}, \underset{\sim}{2}, \ldots, \underset{\sim}{N}) d^3\underset{\sim}{1} d^3\underset{\sim}{2}, \ldots, d^3\underset{\sim}{N}. \tag{1.8}$$

With the normalization used here

$$n_2(\underset{\sim}{1}, \underset{\sim}{2}) \to \frac{N(N-1)}{\Omega^2} \approx \nu^2, \tag{1.9}$$

for

$$|\underset{\sim}{1} - \underset{\sim}{2}| \to \infty, \tag{1.10}$$

where ν is the density. At sufficiently low densities an expansion of the pair distribution function in powers of the activity, z, can be made:[4]

$$n_2(\underset{\sim}{1}, \underset{\sim}{2}) = \lambda^{-6} \sum_{\ell=1}^{\infty} \ell b_\ell(\underset{\sim}{1}, \underset{\sim}{2}) z^{\ell+1}, \tag{1.11}$$

where we use the following definition of z:

$$z = \frac{Q_{N-1}}{Q_N} . \tag{1.12}$$

The functions b_ℓ are modified cluster integrals; for $\ell=1$ and $\ell=2$ they are given by

$$b_1(\underset{\sim}{1}, \underset{\sim}{2}) = W_2(\underset{\sim}{1}, \underset{\sim}{2}), \tag{1.13}$$

$$b_2(\underset{\sim}{1}, \underset{\sim}{2}) = \frac{1}{2\lambda^3}\left\{ \int \left[W_3(\underset{\sim}{1}, \underset{\sim}{2}, \underset{\sim}{3}) - W_2(\underset{\sim}{1}, \underset{\sim}{2}) W_1(\underset{\sim}{3}) \right] d^3\underset{\sim}{3} \right\}. \tag{1.14}$$

At very low densities the activity is approximated by

$$z \approx \nu \lambda^3 \tag{1.15}$$

and, using just the first term in Eq. (1.11),

$$n_2(\underset{\sim}{1}, \underset{\sim}{2}) \approx \nu^2 W_2(\underset{\sim}{1}, \underset{\sim}{2}). \tag{1.16}$$

Because of spherical symmetry in the interaction, Eq. (1.5), $W_2(\underset{\sim}{1}, \underset{\sim}{2})$ depends only on

$$S = |\underset{\sim}{1} - \underset{\sim}{2}|, \tag{1.17}$$

and so we may write

$$W_2(\underset{\sim}{1}, \underset{\sim}{2}) = W_2(S). \tag{1.18}$$

It is tacitly assumed here that Ω is so large that boundary effects can be ignored. The radial distribution function, $g(S)$, in the approximation represented in Eq. (1.16), is given by

$$g(S) \approx W_2(S). \tag{1.19}$$

Our results can also be used to compute the second virial coefficient, given by

$$B = -2\pi N_0 \int_0^\infty (W_2(S) - 1)S^2 dS, \tag{1.20}$$

where N_0 is Avogadro's number. We have made this calculation and found good agreement with other calculations of B.

A secondary reason for presenting this work is to illustrate the use of Wiener integrals as a computational tool. Although the Wiener integral formulation has been known for some time it has found relatively little use as a computational tool. The reasons are probably two-fold; although it has been known, it has not been well known, and the computational labor is enormous. Modern computing equipment is helping break down the second barrier and we hope that this work will help break down the first.

2. PATH INTEGRAL FORMULATION FOR THE SLATER SUM

The path integrals, or more explicitly, the conditional Wiener integrals in terms of which we express the Slater sum, may be defined in the following way. Let the parameter τ be defined on the interval $(0, \beta)$ and let

$$\underset{\sim}{r}(\tau) = (x_1(\tau), y_1(\tau), z_1(\tau), \ldots, x_N(\tau), y_N(\tau), z_N(\tau)) \tag{2.1}$$

denote a continuous function of τ, with the condition $\underset{\sim}{r}(0) = 0$; it is convenient to picture $\underset{\sim}{r}(\tau)$ as the generator of a path in the 3N-dimensional coordinate space of the system as τ goes from 0 to β. Let $F[\underset{\sim}{r}(\tau)]$ denote a functional of $\underset{\sim}{r}(\tau)$. Finally, let

$$\underset{\sim}{r}(\tau;n) = (x_1(\tau;n), y_1(\tau;n), z_1(\tau;n), \ldots, x_N(\tau;n), y_N(\tau;n), z_N(\tau;n)) \tag{2.2}$$

denote an $\underset{\sim}{r}(\tau)$ which is piecewise straight and has breaks at $\tau_1, \tau_2, \ldots, \tau_{n-1}$; such a function is displayed in Fig. 1 for n = 4 and one space coordinate. The end-points of the τ-interval are

$$\tau_0 = 0, \qquad \tau_n = \beta. \tag{2.3}$$

The conditional Wiener integral, $E\{F|\underset{\sim}{r}(\beta) = \underset{\sim}{R}\}$, of the functional $F[\underset{\sim}{r}(\tau)]$ is defined by

$$E\{F|\underset{\sim}{r}(\beta) = R\} = \lim_{n\to\infty} \int_{-\infty}^{+\infty} \cdots \int_{-\infty}^{+\infty} F[\underset{\sim}{r}(\tau;n)]d\mu_n, \tag{2.4}$$

where

$$d\mu_n = A_n \prod_{i=0}^{n-1} \left\{ (2\pi(\tau_{i+1} - \tau_i))^{-\frac{3N}{2}} \exp\left(\frac{-(\underset{\sim}{r}_{i+1} - \underset{\sim}{r}_i)^2}{2(\tau_{i+1} - \tau_i)} \right) \right\} \prod_{i=1}^{n-1} d^{3N}\underset{\sim}{r}_i; \tag{2.5}$$

$$\begin{aligned}(\underset{\sim}{r}_{i+1} - \underset{\sim}{r}_i)^2 = \sum_{j=1}^{N} \Big\{ &(x_j(\tau_{i+1};n) - x_j(\tau_i;n))^2 + (y_j(\tau_{i+1};n) - y_j(\tau_i;n))^2 \\ &+ (z_j(\tau_{i+1};n) - z_j(\tau_i;n))^2 \Big\} ;\end{aligned} \tag{2.6}$$

$$d^{3N}\underset{\sim}{r}_i = \prod_{j=1}^{N} dx_j(\tau_i;n)\, dy_j(\tau_i;n)\, dz_j(\tau_i;n); \tag{2.7}$$

and A_n is chosen so that

$$\int_{-\infty}^{+\infty} \cdots \int_{-\infty}^{+\infty} d\mu_n = 1. \tag{2.8}$$

Piecewise continuity of $F[\underset{\sim}{r}(\tau)]$ is sufficient to ensure the existence of the limit in Eq. (2.4), and we will assume that this sufficiency condition is satisfied.

We wish to draw attention to two features exhibited in the above relations. The measure $d\mu_n$ is a Gaussian probability and so one may loosely regard the conditional Wiener integral as an average of the functional F, where the average is taken over all paths $\underset{\sim}{r}(\tau)$, with the property $\underset{\sim}{r}(0) = 0$, $\underset{\sim}{r}(\beta) = \underset{\sim}{R}$; the statistical weight of a path being characterized by the fact that the infinitesimal increments $\underset{\sim}{r}(\tau + \delta\tau) - \underset{\sim}{r}(\tau)$ are governed by a Gaussian distribution. The measure $d\mu_n$ is invariant to the transformation

$$\tau' \rightarrow \tau, \ \underset{\sim}{r}'(\tau') \rightarrow \underset{\sim}{r}(\tau), \tag{2.9}$$

where

$$\underset{\sim}{r}(\tau) = \sqrt{\alpha} r'(\tau'), \tag{2.10}$$

$$\tau = \alpha \, \tau'. \tag{2.11}$$

Hence the τ-interval can always be normalized to (0, 1) by a change in the space coordinates.

The basic relation connecting the conditional Wiener integral to the Slater sum is[3]

$$(2\pi\beta)^{-\frac{3N}{2}} \exp\left(-\frac{(\underset{\sim}{R}' - \underset{\sim}{R})^2}{2\beta}\right) E\{\exp\,(-\int_0^\beta V_N(\underset{\sim}{r}(\tau) + \underset{\sim}{R})d\tau) | \underset{\sim}{r}(\beta) = \underset{\sim}{R}' - \underset{\sim}{R}\} \tag{2.12}$$

$$= \sum_i \Psi_i^*(\underset{\sim}{R})\Psi_i(\underset{\sim}{R}')\, e^{-\beta E_i},$$

where on the left the τ-interval is $(0,\beta)$, $\underset{\sim}{R}$, $\underset{\sim}{R}'$ are two points in the 3N-dimensional coordinate space, and $(\underset{\sim}{R}' - \underset{\sim}{R})^2$ is the square of the distance between them (cf. Eq. (2.6)); and on the right the sum extends over all eigenstates, characterized by eigenvectors Ψ_i and eigenvalues E_i of the equation

$$\frac{1}{2}\left(\sum_{i=1}^{N} \frac{\partial^2}{\partial x_i^2} + \frac{\partial^2}{\partial y_i^2} + \frac{\partial^2}{\partial z_i^2}\right) \Psi + (E - V_N)\, \Psi = 0, \tag{2.13}$$

where V_N is required to give a discrete spectrum.

Equation (2.13) is the Schrödinger equation in units chosen to make $m = \hbar = 1$, and we now adopt these units; the thermal wave length is now $\sqrt{2\pi\beta}$. It is to be noted that the potential energy, V_N, appears in the functional

$$F[\underset{\sim}{r}(\tau)] = \exp\left(-\int_0^\beta V_N(\underset{\sim}{r}(\tau) + \underset{\sim}{R})d\tau\right), \tag{2.14}$$

which is averaged over all paths. Because $\underset{\sim}{r}(\tau) + \underset{\sim}{R}$ appears in the argument of V_N, we may picture the effective path as one in which the system goes from point $\underset{\sim}{R}$ to point $\underset{\sim}{R}'$ in the τ-interval $(0,\beta)$. This picture appears again when it is recognized that the two sides of Eq. (2.12) are two ways of writing the Green's function for the Bloch equation

$$H_N\, \Phi = \frac{\partial \Phi}{\partial \beta}\ . \tag{2.15}$$

The above formulation ignores symmetry conditions on the eigenfunctions. Taking these conditions into consideration, let P denote the permutation operator, and construct symmetric and antisymmetric eigenfunctions,

$$\Psi_{s,j} = \frac{1}{\sqrt{N!}} \sum_P P\, \Psi_j(\underset{\sim}{R}), \tag{2.16}$$

$$\Psi_{a,j} = \frac{1}{\sqrt{N!}} \sum_P \sigma_P\, P\, \Psi_j(\underset{\sim}{R}), \tag{2.17}$$

where $\sigma_P = +1$ or -1 according as the permutation is even or odd. Now by applying P to both sides of Eq. (2.12), with the convention that P operates on the primed coordinates, and summing over P, one obtains

$$\frac{1}{\sqrt{N!}} \sum_P P(2\pi\beta)^{-\frac{3N}{2}} \exp\left(- \frac{(\underset{\sim}{R}' - \underset{\sim}{R})^2}{2\beta}\right) E\{\exp\,(- \int_0^\beta V_N(\underset{\sim}{r}(\tau) + \underset{\sim}{R})d\tau) | \underset{\sim}{r}(\beta) = \underset{\sim}{R}' - \underset{\sim}{R}\}$$

$$= \sum_j \Psi_j^*(\underset{\sim}{R})\, \Psi_{s,j}\, e^{-\beta E_j}, \tag{2.18}$$

$$\frac{1}{\sqrt{N!}} \sum_P \sigma_P P(2\pi\beta)^{-\frac{3N}{2}} \exp\left(- \frac{(\underset{\sim}{R}' - \underset{\sim}{R})^2}{2\beta}\right) E\{\exp(- \int_0^\beta V_N(\underset{\sim}{r}(\tau) + \underset{\sim}{R})d\tau) | \underset{\sim}{r}(\beta) = \underset{\sim}{R}' - \underset{\sim}{R}\}$$

$$= \sum_j \Psi_j^*(\underset{\sim}{R}) \Psi_{a,j}\, e^{-\beta E_j}. \tag{2.19}$$

We now impose the requirement that $\underset{\sim}{R}$ be a point derived from $\underset{\sim}{R}'$ by some permutation of the particle coordinates. Noting that for any E_j there are N! Ψ_j's because of the symmetry degeneracy, and that in a sum over these Ψ_j's, $\Psi_{s,j}$ is constant and $\Psi_{a,j}$ changes sign we have the fundamental relations

$$\sum_P P \exp\left(-\frac{\underset{\sim}{R}' - \underset{\sim}{R})^2}{2\beta}\right)E\{\exp(-\int_0^\beta V_N(\underset{\sim}{r}(\tau) + \underset{\sim}{R})d\tau)|\underset{\sim}{r}(\beta) = \underset{\sim}{R}' - \underset{\sim}{R}\} = W_N^B, \tag{2.20}$$

$$\sum_P \sigma_P P \exp\left(-\frac{(\underset{\sim}{R}' - \underset{\sim}{R})^2}{2\beta}\right)E\{\exp(-\int_0^\beta V_N(\underset{\sim}{r}(\tau) + \underset{\sim}{R})d\tau)|\underset{\sim}{r}(\beta) = \underset{\sim}{R}' - \underset{\sim}{R}\} = W_N^F, \tag{2.21}$$

where W_N^B and W_N^F are the Slater sums for Bose-Einstein and Fermi-Dirac statistics. The relation shown in Eq. (2.20) was used some years ago in a study of the λ-transition of helium.[5]

3. FORMULAS FOR THE CALCULATION OF W_2^B

To compute W_2^B it is convenient to use the center of mass and relative coordinates. The Slater sum separates into the product of two Slater sums, one for the center of mass coordinate $\overline{\underset{\sim}{R}}$, which can be evaluated immediately, and one for the relative coordinate $\underset{\sim}{S}$,

$$W_2 = 2\lambda^6 \int \frac{d^3k}{(2\pi)^3} e^{-i\underset{\sim}{k}\cdot\underset{\sim}{\overline{R}}} e^{-\beta\frac{k^2}{4}} e^{i\underset{\sim}{k}\cdot\underset{\sim}{\overline{R}}} \sum_i \phi_i^*(\underset{\sim}{S})\, \phi_i(\underset{\sim}{S})\, e^{-\beta E_i},$$

$$= 2^{\frac{5}{2}} \lambda^3 \sum_i \phi_i^*(\underset{\sim}{S})\, \phi_i(\underset{\sim}{S})\, e^{-\beta E_i}, \qquad (3.1)$$

where $\phi_i(\underset{\sim}{S})$ satisfies the Schrödinger equation for the relative coordinate,

$$\nabla^2\phi_i(\underset{\sim}{S}) + (E_i - V(\underset{\sim}{S}))\, \phi_i(\underset{\sim}{S}) = 0. \qquad (3.2)$$

The interchange of the two particles does not alter the center of mass coordinate but changes the relative coordinate $\underset{\sim}{S}$ into $-\underset{\sim}{S}$, so

$$W_2^B = W_2^D + W_2^E, \qquad (3.3)$$

$$W_2^F = W_2^D - W_2^E, \qquad (3.4)$$

where the direct term, W_2^D, is given by

$$W_2^D = 2^{\frac{3}{2}} \lambda^3 \sum_i \phi_i^*(\underset{\sim}{S})\phi_i(\underset{\sim}{S})\, e^{-\beta E_i}, \qquad (3.5)$$

and the exchange term W_2^E is

$$W_2^E = 2^{\frac{3}{2}} \lambda^3 \sum_i \phi_i^*(-\underset{\sim}{S})\, \phi_i(\underset{\sim}{S})\, e^{-\beta E_i}. \qquad (3.6)$$

It is to be recognized that the sums in Eqs. (3.5) and (3.6) extend over all states without regard to symmetry. Incorporating the physical constants into Eq. (2.12) and performing the normalization of τ to the interval (0,1) according to Eqs. (2.9), (2.10), and (2.11) one obtains,

$$W_2^D = E\left\{ \exp\left(-\beta\int_0^1 V\left(\frac{\lambda}{\sqrt{\pi}}\underset{\sim}{r}(\tau) + \underset{\sim}{S}\right)d\tau\right) \Big| \underset{\sim}{r}(1) = 0\right\}, \tag{3.7}$$

and

$$W_2^E = e^{-\frac{2\pi S^2}{\lambda^2}}\, E\left\{ \exp\left(-\beta\int_0^1 V\left(\frac{\lambda}{\sqrt{\pi}}\underset{\sim}{r}(\tau) + \underset{\sim}{S}\right)d\tau\right) \Big| \underset{\sim}{r}(1) = -\frac{2\sqrt{\pi}}{\lambda}\underset{\sim}{S}\right\}, \tag{3.8}$$

where $\underset{\sim}{r}(\tau)$ is the generator of the path of the system in the 3-dimensional relative coordinate space as τ goes from 0 to 1. A transformation can be performed on $\underset{\sim}{r}(\tau)$ in Eq. (3.8) to make the condition at $\underset{\sim}{r}(1)$ the same as that in Eq. (3.7). The result is

$$W_2^E = e^{-\frac{2\pi S^2}{\lambda^2}}\, E\left\{ \exp\left(-\beta\int_0^1 V\left(\frac{\lambda}{\sqrt{\pi}}\underset{\sim}{r}(\tau) + \underset{\sim}{S} - 2\tau\underset{\sim}{S}\right)d\tau\right) \Big| \underset{\sim}{r}(1) = 0\right\}. \tag{3.9}$$

Let $F[\underset{\sim}{r}(\tau)]$ denote either of the two functionals,

$$F^D[\underset{\sim}{r}(\tau)] = \exp\left(-\beta\int_0^1 V\left(\frac{\lambda}{\sqrt{\pi}}\underset{\sim}{r}(\tau) + \underset{\sim}{S}\right)d\tau\right), \tag{3.10}$$

or

$$F^E[\underset{\sim}{r}(\tau)] = \exp\left(-\beta\int_0^1 V\left(\frac{\lambda}{\sqrt{\pi}}\underset{\sim}{r}(\tau) + \underset{\sim}{S} - 2\tau\underset{\sim}{S}\right)d\tau\right) . \qquad (3.11)$$

Then the numerical scheme for evaluating the conditional Wiener integrals in Eqs. (3.7) and (3.9) is to approximate each by a 3n-dimensional integral,

$$E\{F|\underset{\sim}{r}(1) = 0\} \approx \int_{-\infty}^{\infty}\cdots\int_{-\infty}^{\infty} F[\underset{\sim}{r}(\tau;n)]d\mu_n, \qquad (3.12)$$

where $d\mu_n$ is given in Eq. (2.5) with $\underset{\sim}{r}_0 = \underset{\sim}{r}_n = 0$. The break points in the piecewise straight path $\underset{\sim}{r}(\tau;n)$ are chosen at equal time intervals, $\tau_i = \frac{i}{n}$, $i = 0, 1, \ldots, n$. The 3n-dimensional integral is then evaluated by a Monte Carlo sampling procedure. The sampling is done by choosing the coordinates of the break points $\underset{\sim}{r}_i = \underset{\sim}{r}(\tau_i;n)$ of $\underset{\sim}{r}(\tau;n)$ according to the distribution $d\mu_n$. $F[\underset{\sim}{r}(\tau;n)]$ is then evaluated with this path for a set of values of $S = |\underset{\sim}{S}|$. Further piecewise straight paths are then chosen and $F[\underset{\sim}{r}(\tau;n)]$ is averaged over all paths for each value of S.

Concerning the choice of the $\underset{\sim}{r}_i$, it is evident that the distribution $d\mu_n$ does not give independent Gaussian increments $(\underset{\sim}{r}_{i+1} - \underset{\sim}{r}_i)$ due to the condition $\underset{\sim}{r}_n = 0$; however, the choice of the $\underset{\sim}{r}_i$ can be made to depend on independent Gaussian random variables by use of an interpolation formula for a conditional Brownian motion path.[6] If $\underset{\sim}{r}_0, \underset{\sim}{r}_1, \ldots, \underset{\sim}{r}_i$ are fixed then,

$$\underset{\sim}{r}_{i+1} = \frac{\underset{\sim}{r}_i(\tau_n - \tau_{i+1}) + \underset{\sim}{r}_n(\tau_{i+1} - \tau_i)}{\tau_n - \tau_i} + \underset{\sim}{\xi}\sqrt{\frac{(\tau_{i+1} - \tau_i)(\tau_n - \tau_{i+1})}{\tau_n - \tau_i}}\,, \qquad (3.13)$$

where the coordinate random variables of $\underset{\sim}{\xi} = (\xi_x, \xi_y, \xi_z)$ are independent and Gaussianly distributed with mean 0 and variance 1.

The labor involved in the evaluation of $F[\underset{\sim}{r}(\tau;n)]$ is reduced by the fact that it is not necessary to evaluate the τ-integral to a high order of accuracy. On the basis of some earlier work[7] we can expect the approximation represented by Eq. (3.12) to have an error not less than $\mathcal{O}\left(\frac{1}{n}\right)$.[8] It is therefore sufficient to evaluate the τ-integral by applying the trapezoidal rule to the intervals (τ_{i-1}, τ_i), $i = 1, 2, \ldots, n$. Then,

$$F^D[\underset{\sim}{r}(\tau;n)] \approx \exp\left(-\frac{\beta}{n} \sum_{i=0}^{n-1} V\left(\frac{\lambda}{\sqrt{\pi}} \underset{\sim}{r}_i + \underset{\sim}{S}\right)\right). \tag{3.14}$$

Let M paths $\underset{\sim}{r}^j(\tau;n)$, $j = 1, 2, \ldots, M$ be chosen according to the sampling scheme described above, let V be given by Eq. (1.5), and introduce the dimensionless variables,

$$\rho = \frac{\sigma\sqrt{\pi}}{\lambda}, \quad \gamma = 4\alpha\beta, \quad \underset{\sim}{d} = \frac{\underset{\sim}{S}\sqrt{\pi}}{\lambda}. \tag{3.15}$$

Then the numerical approximations to W_2^D and W_2^E are given explicitly by the formulas,

$$W_2^D \approx \frac{1}{M} \sum_{j=1}^{M} \exp\left[-\frac{\gamma}{n} \sum_{i=0}^{n-1} \left(\left(\frac{\underset{\sim}{r}_i^j + \underset{\sim}{d}}{\rho}\right)^{-12} - \left(\frac{\underset{\sim}{r}_i^j + \underset{\sim}{d}}{\rho}\right)^{-6}\right)\right] \tag{3.16}$$

and

$$W_2^E \approx \frac{1}{M} \sum_{j=1}^{M} \exp\left[-\frac{\gamma}{n} \sum_{i=0}^{n-1} \left(\left(\frac{\underset{\sim}{r}_i^j + \underset{\sim}{d}(1-2\tau_i)}{\rho} \right)^{-12} - \left(\frac{\underset{\sim}{r}_i^j + \underset{\sim}{d}(1-2\tau_i)}{\rho} \right)^{-6} \right) \right]. \tag{3.17}$$

4. RESULTS OF THE CALCULATION OF W_2^B

It is evident from the formulas in the last section that they approach the classical result when the thermal wave length vanishes; i.e., when λ → 0, Eqs. (3.7) and (3.8) give

$$W_2^D \to \exp\,(-\beta V(\underset{\sim}{S})), \tag{4.1}$$

$$W_2^E \to 0. \tag{4.2}$$

One can see from a simple qualitative argument that for fixed n the approximation, Eq. (3.12), is expected to improve as λ → 0. In this approximation the true ensemble of paths has been replaced by an ensemble of broken straight line paths, one straight line segment in such a path corresponding to a "time" interval of $\frac{1}{n}$ in length. If we consider a finer subdivision, obtained by chopping each of the n intervals in half, then each straight line segment will have a break at the center as illustrated in Fig. 2 for one space coordinate. We can now think of the deviation, ξ, at the center of the first interval in Fig. 2 as a random variable. From the interpolation formula, Eq. (3.13), it follows that it may be regarded as a Gaussian random variable with variance $\frac{1}{4n}$. Thus in our original approximation, with time segments $\frac{1}{n}$, we are, roughly speaking, ignoring fluctuations in each space coordinate of the order

$$\frac{\lambda}{\sqrt{\pi}} \cdot \sqrt{\frac{1}{4n}} \, ;$$

the factor $\frac{\lambda}{\sqrt{\pi}}$ enters because it multiplies the path coordinate in Eqs. (3.7) and (3.8). It is therefore reasonable to assume that the accuracy of our approximation will improve as $\lambda \to 0$. Conversely, we can expect a larger error as $\lambda \to \infty$; i.e., as the temperature becomes small. The above argument suggests that a decrease in temperature must be compensated by an increase in n such that Tn remains constant, if the error is to remain constant as the temperature is lowered. Since the computing time depends critically on n, it is clear that one cannot expect to pursue these calculations to arbitrarily low temperatures.

Computing time restrictions led us to use the value

$$n = 512 = 2^9 \qquad (4.3)$$

in almost all of the calculations. It is extremely difficult to get an a priori estimate of the error to be expected for a given temperature and value of n. However, one can get a useful picture of the error in the following way. As a consequence of the argument in the last paragraph we certainly must restrict our attention to temperatures such that fluctuations in position of the order

$$\frac{\lambda}{\sqrt{\pi}} \cdot \sqrt{\frac{1}{4n}} = 2^{-5} \sqrt{\beta} \qquad (4.4)$$

are small compared with the range of the potential. Retaining 0.1% (relative to the potential minimum) accuracy in the potential then, from Eq. (1.9), it is reasonable to regard the range of V as 4σ ; i.e., to regard V = 0 for $r > 4\sigma$. Hence our criterion becomes:

$$\frac{2^{-7}\sqrt{\beta}}{\sigma}$$

must be small, relative to unity, or, substituting the values of k and σ, $\frac{0.03}{\sqrt{T}}$ must be small relative to unity. This crude argument ignores the fact that V changes very rapidly when $\frac{r}{\sigma} < 1$, however this neglect is not so serious as it might appear since $e^{-\beta V}$ is practically zero for these values of r.

Except at low temperatures, the exchange term W_2^E should be small. An estimate of the upper bound for this term is easy to construct from the present formulation. To get this estimate we make a slight change in the potential and insist that $V(r) = \infty$ for $r < \sigma$ and otherwise is given by Eq. (1.5). Under this condition the Wiener integral factor in Eq. (3.9) is zero for $|S| < \sigma$ and cannot exceed $e^{\beta\alpha}$ for $|S| \geq \sigma$. It follows that W_2^E, for this modified potential, satisfies the inequality[9]

$$W_2^E \leq e^{-\frac{2\pi\sigma^2}{\lambda^2} + \beta\alpha} , \qquad (4.5)$$

and substitution of the values of the physical constants gives

$$W_2^E \le e^{-0.54T + \frac{10}{T}} \tag{4.6}$$

Our results show that W_2^E is considerably smaller than this bound. The most likely explanation for this is the following one. Examination of Eq. (3.9) shows that at the midpoint of the path ($\tau = \frac{1}{2}$) the potential is

$$V(\frac{\lambda}{\sqrt{\pi}} \underset{\sim}{r}(\tfrac{1}{2})),$$

therefore it can be expected that the Wiener integral in Eq. (3.9) will be very small except when λ is large enough to make

$$\frac{\lambda^2}{\pi} r^2(\tfrac{1}{2}) > \sigma^2 \tag{4.7}$$

with a nonvanishing probability. If we simply replace $r^2(\frac{1}{2})$ by its mean value, $\frac{3}{4}$ (see Eq. (3.13)), this inequality becomes

$$T < 2.8^\circ \text{ K}. \tag{4.8}$$

This argument suggests that we can only expect a significant contribution from the exchange term below 2.8° K, and our numerical results support this conclusion. This argument points to an interesting picture of contributions to the exchange term. One contribution comes from the exponential factor which, as we have seen, introduces a factor of

$$e^{-\frac{2\pi\sigma^2}{\lambda^2}}$$

in the bound. Thus this factor will make the exchange term go to zero like e^{-kT} as $T \to \infty$. One can picture this contribution as coming from the kinetic energy associated with the relative motion when the particles exchange position. Another contribution comes from the interaction during the exchange in position and this contribution also makes the exchange term vanish as $T \to \infty$; see Fig. 3. Our results suggest that the latter effect is probably more important than the kinetic energy effect in making the exchange term small.

In Fig. 4 the Slater sum, W_2^B, as a function of $\frac{S}{\sigma}$ for different temperatures is displayed. Some results have been omitted to improve the legibility of this figure. Only the curve for $T = 2^\circ$ K explicitly includes the exchange term. At $T = 5^\circ$ K the exchange term was found to be negligible compared with the direct term so it was not calculated for the higher temperatures and is omitted in the results for $T = 5^\circ$ K and above. The location and height of the maximum is given in Table I.

There are two important sources of error in these calculations, one arising from the Monte Carlo sampling and the other arising from the approximation represented in Eq. (3.12). For reasons just discussed it is to be expected that these errors will be most important at lower temperatures. A measure of the Monte Carlo sampling error is shown in Figs. 5a and b where the calculated points with standard deviations are shown for $T = 5^\circ$ K and 30° K. The length of the vertical line at a point is twice the standard

deviation of the sample consisting of 1000 independent paths. Standard deviations are not shown in the tails where they are too small to draw on this scale. Some measure of the other error is given by comparing results based on other values of n, the number of straight line segments in the path. In Fig. 6 the results of calculating W_2^D (the direct term) at $T = 2^\circ$ K for n = 100 and n = 512 are shown.

In our initial calculations we only went down to $T = 5^\circ$ K because we suspected that the errors encountered at lower temperatures would be too large. After learning[10] that Larsen and Kilpatrick had calculated W_2^B at $T = 2^\circ$ K in an entirely different way we were stimulated to push our calculations down to 2° K. The results compared with those of Larsen and Kilpatrick are shown in Figs. 7a and b; the direct term is shown in Fig. 7a and the exchange term is shown in Fig. 7b. The sampling error at a representative set of points is shown.

It is of some interest to compare these results against the pure classical value of W_2 and its value from the first few terms of an expansion[11] in powers of λ, sometimes called the Wigner-Kirkwood expansion. The classical value is given by

$$W_2(\text{classical}) = e^{-\beta V}. \tag{4.9}$$

The Wigner-Kirkwood value displayed here is obtained by truncating the expansion at terms in $\frac{1}{S^{14}}$ to obtain

$$W_2(\text{W-K}) = W_2(\text{classical}) \cdot C, \tag{4.10}$$

where

$$C = \exp\left(2.5 \frac{\gamma}{\rho^2} \left(\frac{\sigma}{S}\right)^8 + 7.0 \frac{\gamma}{\rho^4} \left(\frac{\sigma}{S}\right)^{10} + \left(1.5 \frac{\gamma^2}{\rho^2} - 11 \frac{\gamma}{\rho^2}\right)\left(\frac{\sigma}{S}\right)^{14}\right), \qquad (4.11)$$

and where γ and ρ are given in Eq. (3.15). This comparison is made in Figs. 8a,b,c at T = 2° , 10°, and 30° K. Only the direct term is shown.

One cannot of course expect good agreement but it is nevertheless tempting to compare the radial distribution function in the present approximation against experimental results. This comparison is made in Table II where we compare location and height of the first maximum in g(S) and the point at which g(S) first increases above zero for He_4 according to measurements by Henshaw[12] with our results. We note that although there is a marked difference in the height of the maximum, the other parameters are in fairly good agreement. It is to be noted that the position of the maximum moves to higher S as the temperature increases while our results show the opposite behavior. This qualitative difference is almost certainly due to the fact that the approximation used here, Eq. (1.19), includes no dependence on density. Henshaw's measurements were taken at T = 2.2° K, density = 0.146 gm/cm^3 and T = 5.04° K, density = 0.095 gm/cm^3.

The second virial coefficient, Eq. (1.20), obtained from our calculations is compared with results by Kilpatrick, Keller, Hammel and Metropolis[13] in Table III. The results marked by an e were obtained by us using the high temperature expansion.[14] Experimental results are displayed in column 4.

ACKNOWLEDGMENTS

We wish to thank Dr. Sigurd Larsen for communicating his results to us and for an interesting conversation. Some of this work was done while one of us (L. D. F.) had a Fellowship from the John Simon Guggenheim Memorial Foundation and was located at the Max Planck Institut für Physik und Astrophysik in Munich. He wishes to thank the foundation for its support and the Institut for its hospitality.

T($^\circ$ K)	Max W_2^B	$\frac{S}{\sigma}$
2	1.94	1.52
5	1.55	1.46
10	1.40	1.39
20	1.28	1.31
30	1.22	1.27
40	1.18	1.24
50	1.15	1.22
75	1.11	1.19
100	1.09	1.18
273.18	1.04	1.14

Table I: Maximum value of W_2^B (column 2) and the location of this maximum (column 3) for different temperatures (column 1).

$T(^\circ K)$	Position where g(S) rises from zero (A)		Position of maximum in g(S) (A)		Height of maximum of g(S)	
	This Work	Henshaw	This Work	Henshaw	This Work	Henshaw
2°	2.1	2.25	3.89	3.70	1.94	1.4
5°	2.1	2.20	3.74	3.94	1.55	1.3

Table II: Comparison of parameters of g(S), the pair distribution function according to the present calculations, using the approximation of Eq. (1.19), and the experimental results of Henshaw (footnote reference 12, Table I, lines 1 and 3).

T(° K)	B		
	This Work	Kilpatrick et al	Experiment
2	-182.84	-177.39	-193.3 [a]
5	- 59.41	- 59.14	- 62.2 [b]
10	- 21.30	- 21.34	- 23.4 [b]
20	- 2.49	- 2.53	- 4.04 [b]
30	3.68	3.57	2.42 [b]
40	6.59	6.49	6.57(40.09°K)[c]
50	8.26	8.16	8.06(50.09°K)[c]
75	10.28	10.14[e]	10.70(75.01°K)[c]
100	11.08	11.02[e]	11.85(100.02°K)[c]
273.18	11.65	11.59[e]	11.77 [d]

Table III: The second virial coefficient compared with the computer results of Kilpatrick, Keller, Hammel and Metropolis and with experiment.

a. Obtained by linear extrapolation of the data in W. E. Keller, Phys. Rev. 97, 1 (1955).

b. David White, Thor Rubin, Paul Camky and H. L. Johnson, J. Phys. Chem., 64, 1607 (1960).

c. W. H. Keesom, Helium (Elsevier, Amsterdam 1942).

d. W. G. Schneider and J. A. H. Duffie, J. Chem. Phys. 17, 751 (1949).

e. Obtained by us from the high temperature expansion (footnote reference 14).

FOOTNOTES

† This work was supported in part by the Office of Naval Research under Contract Nonr-1834(27).

[1] Contrary to custom we include the multiplying factor $N!\,\lambda^{3N}$ in this definition.

[2] J. deBoer and A.Michels, Physica 6, 409 (1939).

[3] M. Kac, *Lectures in Applied Mathematics, Volume 1, Proceedings of the Summer Seminar, Boulder, Colorado, 1957*, (Interscience Publishers, Inc., New York, 1958).

[4] J. deBoer, Reports on Progress in Physics, London, 12, 305 (1949).

[5] R. P. Feynman, Phys. Rev. 91, 1291 (1953).

[6] P. Levy, *Le Mouvement Brownien*, Memor., Sci. Math. Fasc. 126, Gauthier-Villars, Paris, 1954.

[7] Lloyd D. Fosdick, Mathematics of Computation 19, 225 (1965).

[8] Since the Lennard-Jones potential at $r = 0$ does not satisfy the conditions required in footnote reference 7, we cannot say with certainty that the error is $\mathcal{O}(\frac{1}{n})$ but only that it is not likely to go to zero faster than $\frac{1}{n}$.

[9] This bound has also been discussed in a report by Sigurd Yves Larsen, John E. Kilpatrick, Elliott H. Lieb, and Harry F. Jordan.

[10] Private communication. The calculation of Larsen and Kilpatrick is based on a direct calculation of the wave functions which had been made earlier in a calculation of the second virial coefficient of He_4.

[11] D. ter Haar, Elements of Statistical Mechanics, (Holt, Rinehart and Winston, New York, 1960), p. 192.

[12] D. G. Henshaw, Phys. Rev. 119, 14 (1965).

[13] John E. Kilpatrick, William E. Keller, Edward F. Hammel, and Nicholas Metropolis, Phys. Rev. 94, 1103 (1954).

[14] J. O. Hirschfelder, R. B. Bird, C. F. Curtiss, Molecular Theory of Gases and Liquids, (John Wiley and Sons, Inc., New York, 1954), p. 1119.

FIGURE CAPTIONS

Figure 1: Example of $x(\tau;4)$.

Figure 2: Illustration of the error in using paths $x(\tau;4)$. Fluctuations represented by ξ are ignored.

Figure 3: Two-dimensional illustration of the qualitative difference between a high temperature exchange path and a low temperature exchange path (relative coordinates). As the temperature becomes higher the path tends to follow more closely the straight line connecting points S and -S.

Figure 4: W_2^B as a function of $\frac{S}{\sigma}$ for T = 2° K, 5° K, 10° K, 75° K and 273.18° K.

Figure 5a: W_2^B as a function of $\frac{S}{\sigma}$ for T = 5° K with the Monte Carlo sampling error shown. Total length of the error indicator, represented by the vertical line segment, is twice the standard deviation of the sample mean, represented by the dot.

Figure 5b: W_2^B as a function of $\frac{S}{\sigma}$ for T = 30° K with the Monte Carlo sampling error shown. Total length of the error indicator, represented by the vertical line segment, is twice the standard deviation of the sample mean, represented by the dot.

Figure 6: W_2^D (the direct term) at T = 2° K for n = 100 and n = 512.

Figure 7a: Comparison of our results with those of Larsen and Kilpatrick for the direct term at T = 2° K. The Monte Carlo sampling error (as in Figs. 5a,b) is shown.

FIGURE CAPTIONS (CONT'D)

Figure 7b: Comparison of our results with those of Larsen and Kilpatrick for the exchange term at T = 2° K. The Monte Carlo sampling error (as in Figs. 5a,b) at a representative set of points is shown.

Figure 8a: Comparison of the classical approximation, a Wigner-Kirkwood approximation (Eq. 4.10), and our results for W_2^D at T = 2° K.

Figure 8b: Comparison of the classical approximation, a Wigner-Kirkwood approximation (Eq. 4.10), and our results for W_2^D at T = 10° K.

Figure 8c: Comparison of the classical approximation, a Wigner-Kirkwood approximation (Eq. 4.10), and our results for W_2^D at T = 30° K.

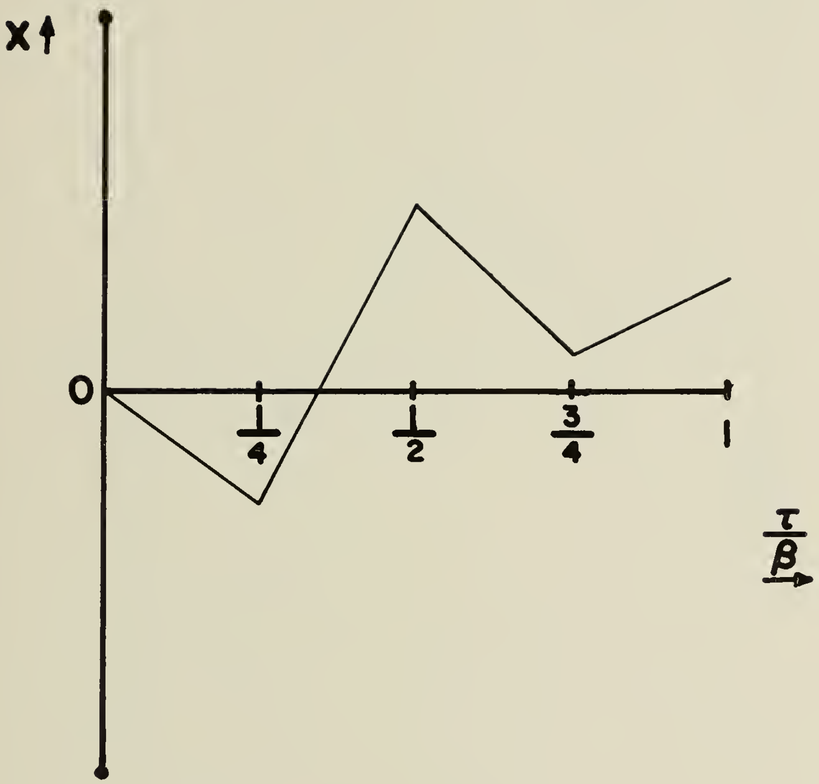

Figure 1.

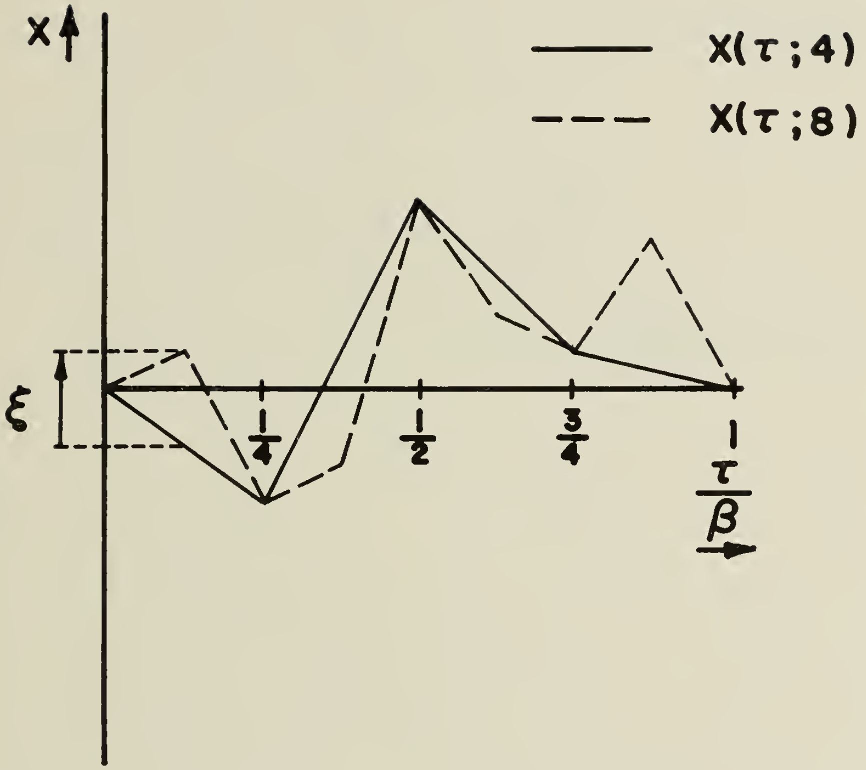

Figure 2.

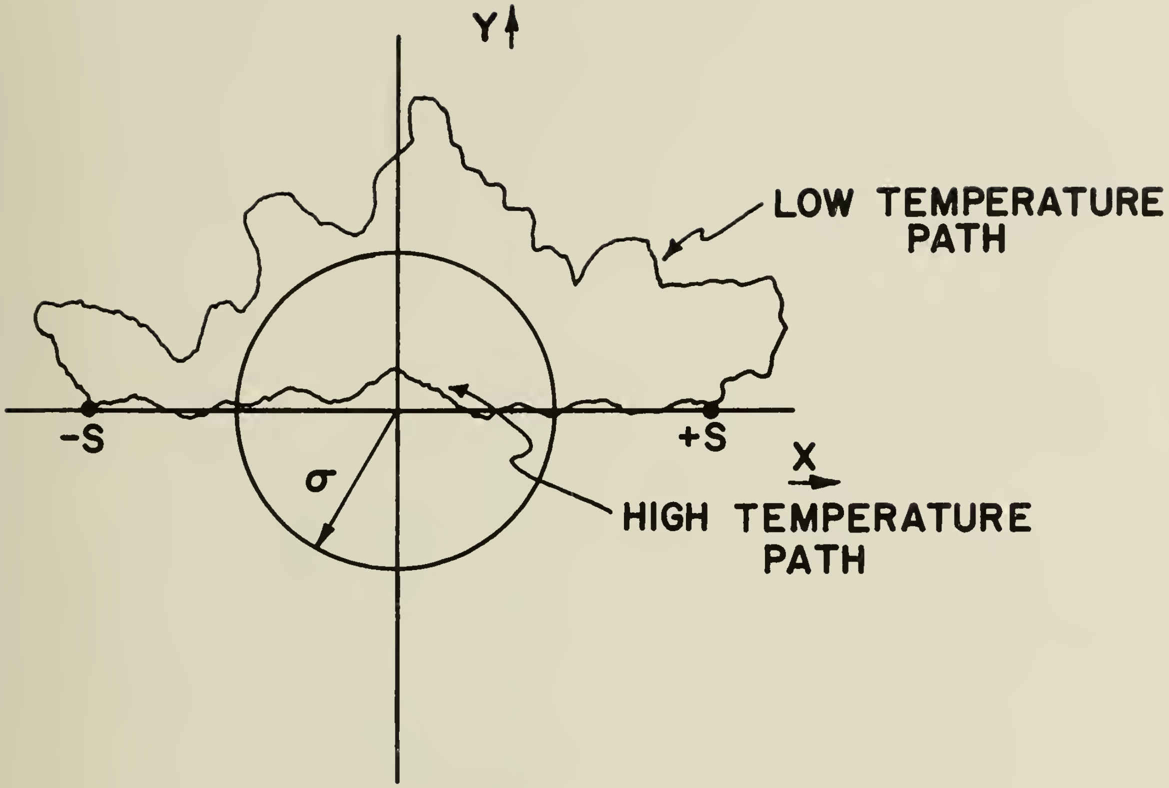

Figure 3.

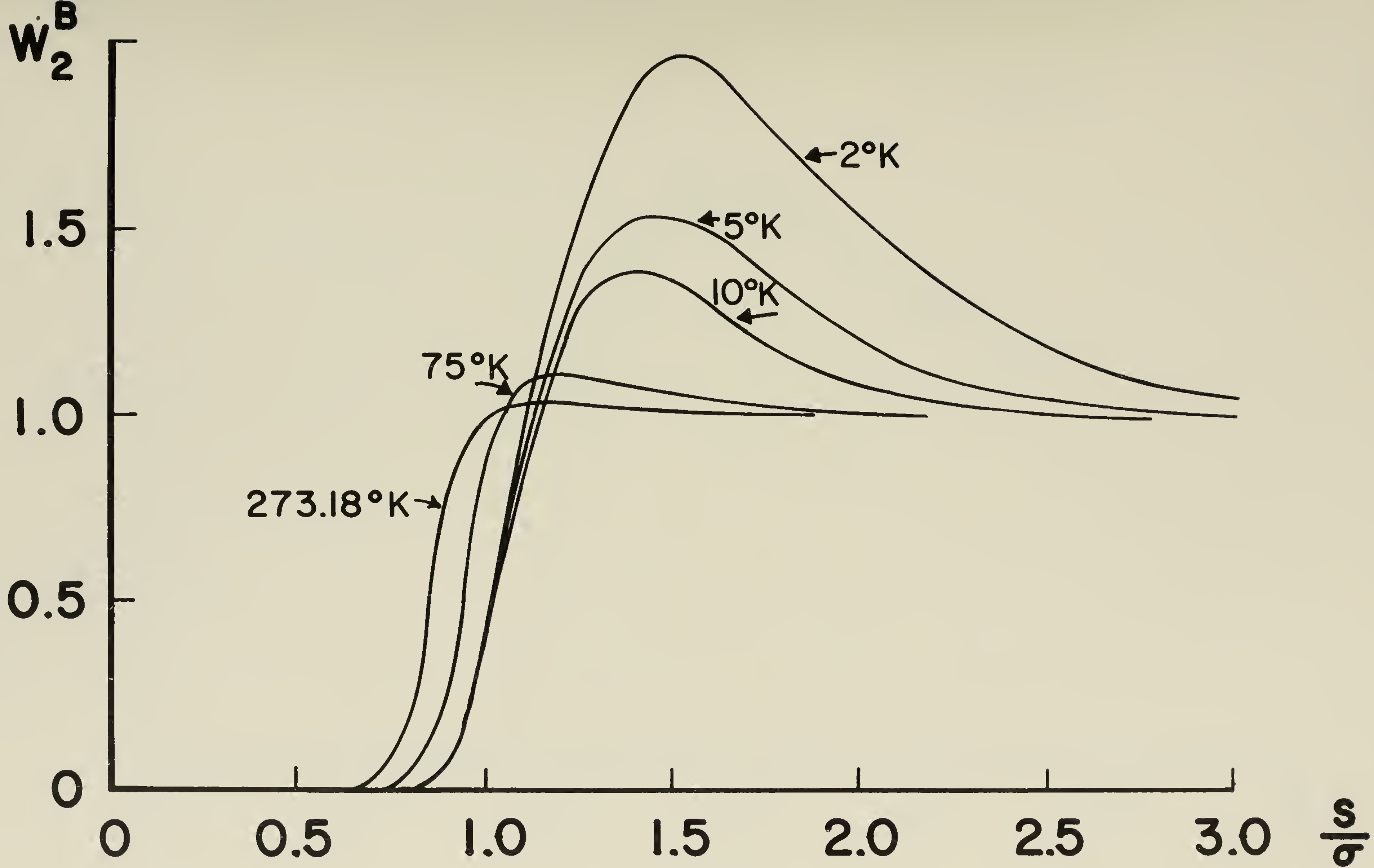

Figure 4.

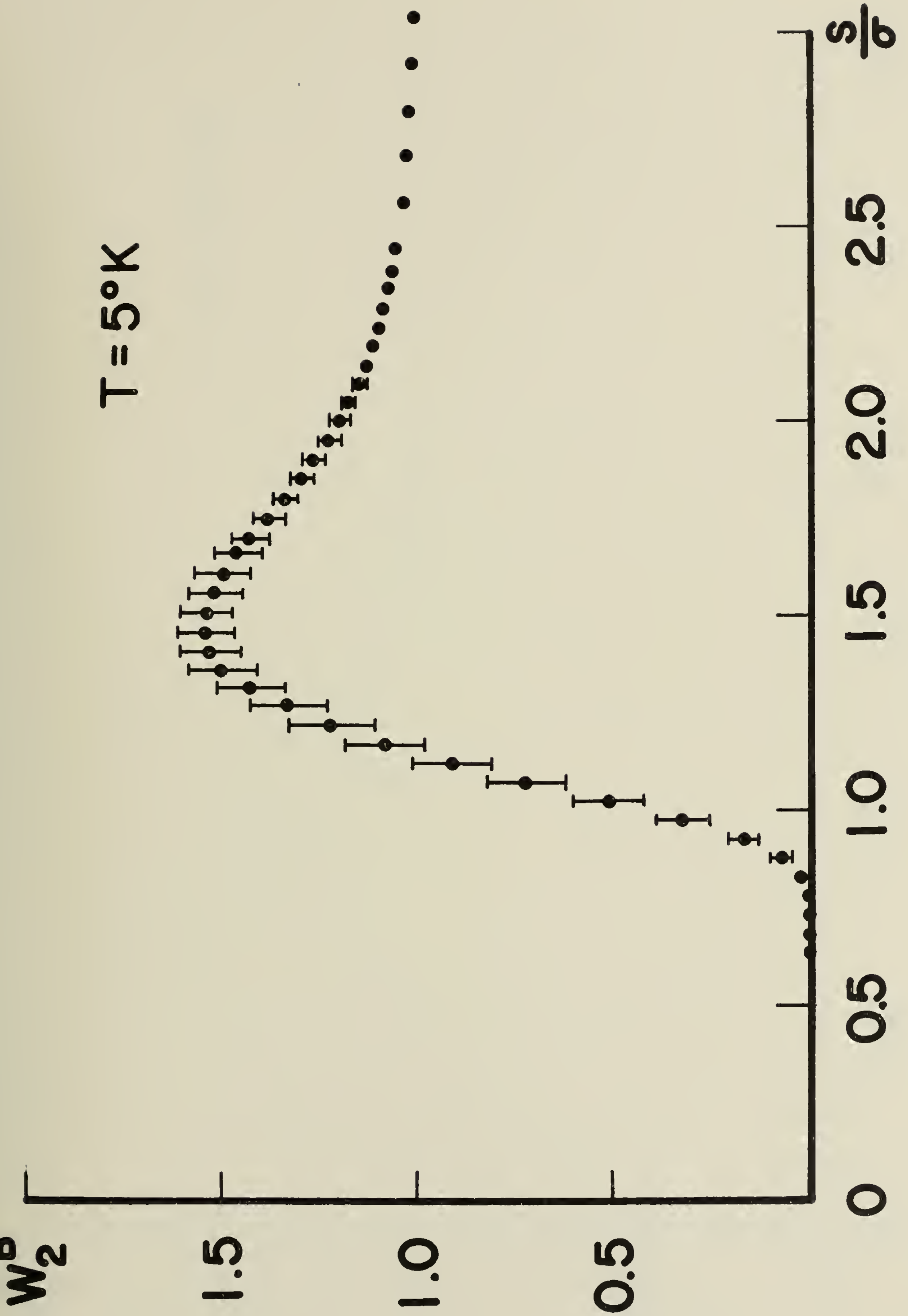

Figure 5a

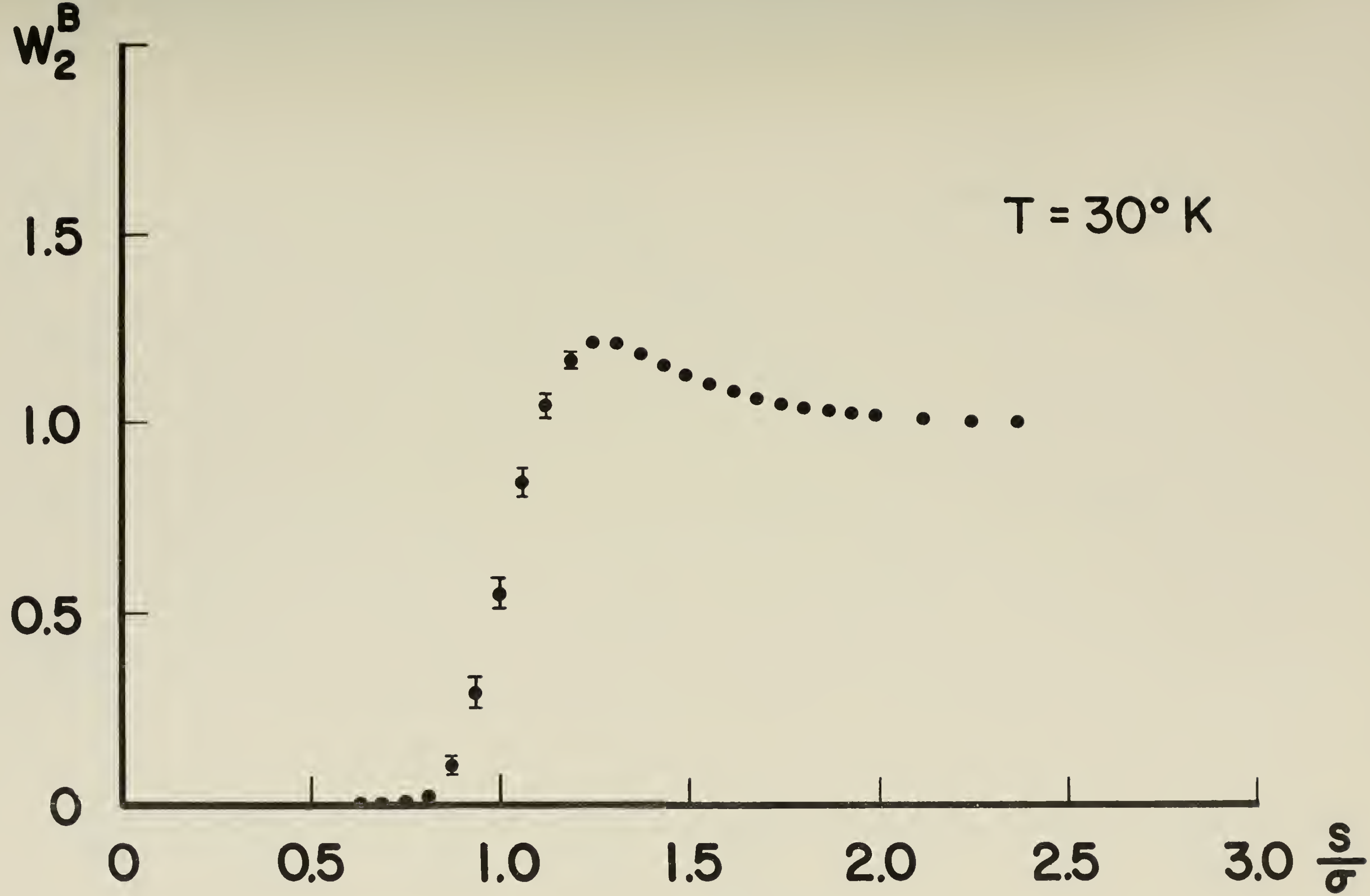

Figure 5b

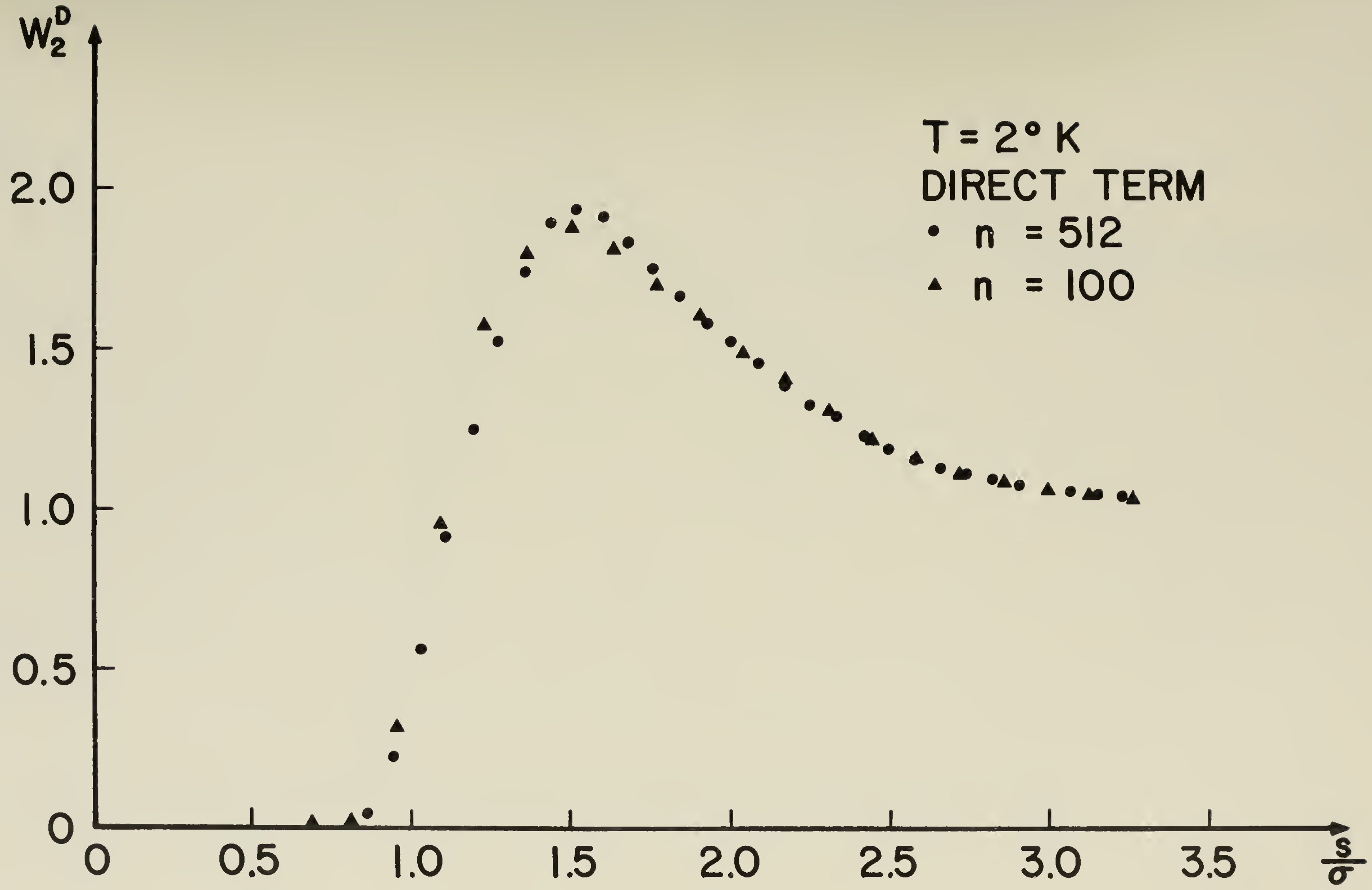
W_2^D
2.0
1.5
1.0
0.5
0
0
0.5
1.0
1.5
2.0
2.5
3.0
3.5
$\frac{s}{\sigma}$
T = 2° K
DIRECT TERM
● n = 512
▲ n = 100

Figure 6

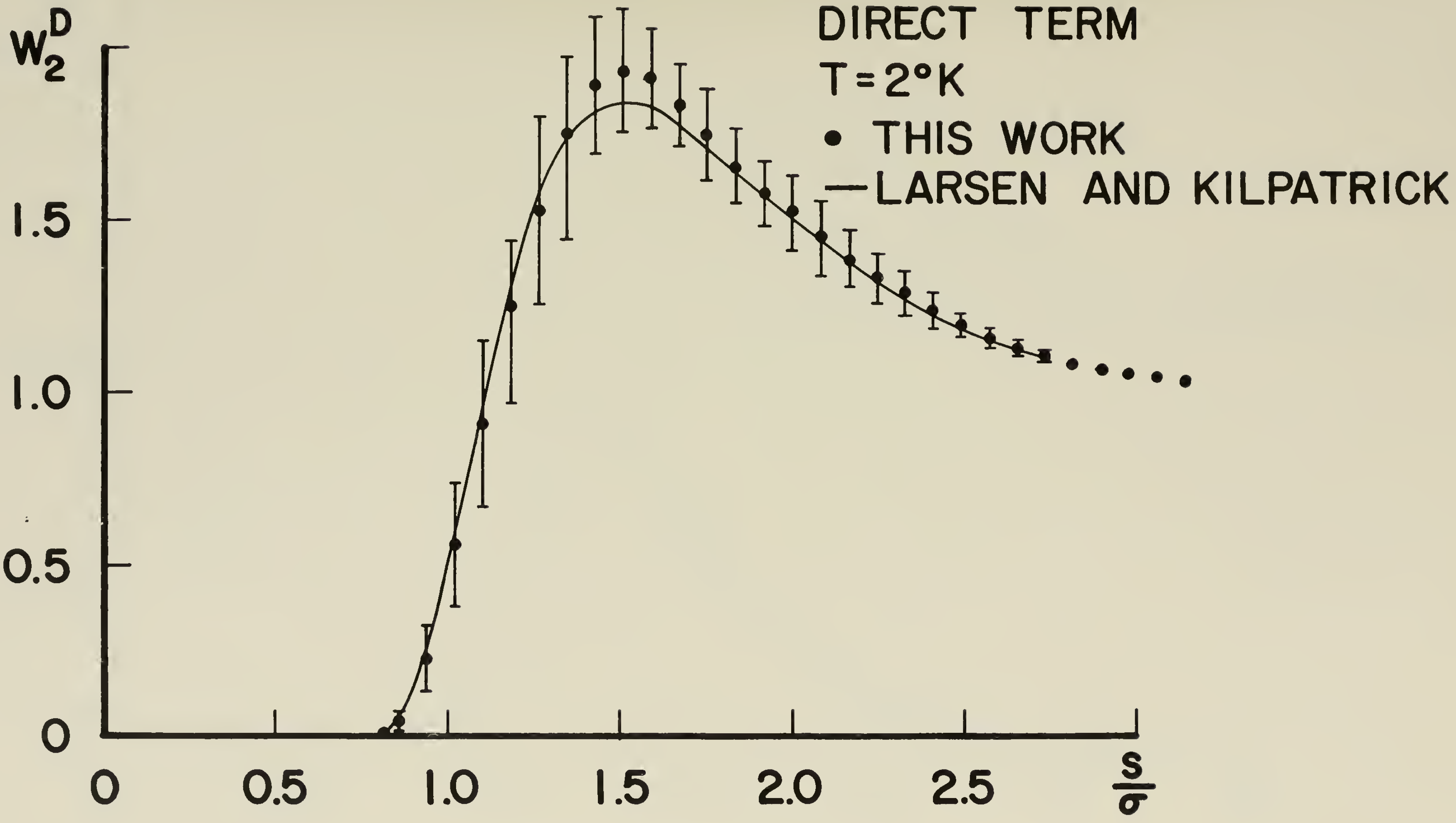
W_2^D
1.5
1.0
0.5
0
0
0.5
1.0
1.5
2.0
2.5
$\frac{s}{\sigma}$
DIRECT TERM
T = 2°K
● THIS WORK
— LARSEN AND KILPATRICK

Figure 7a

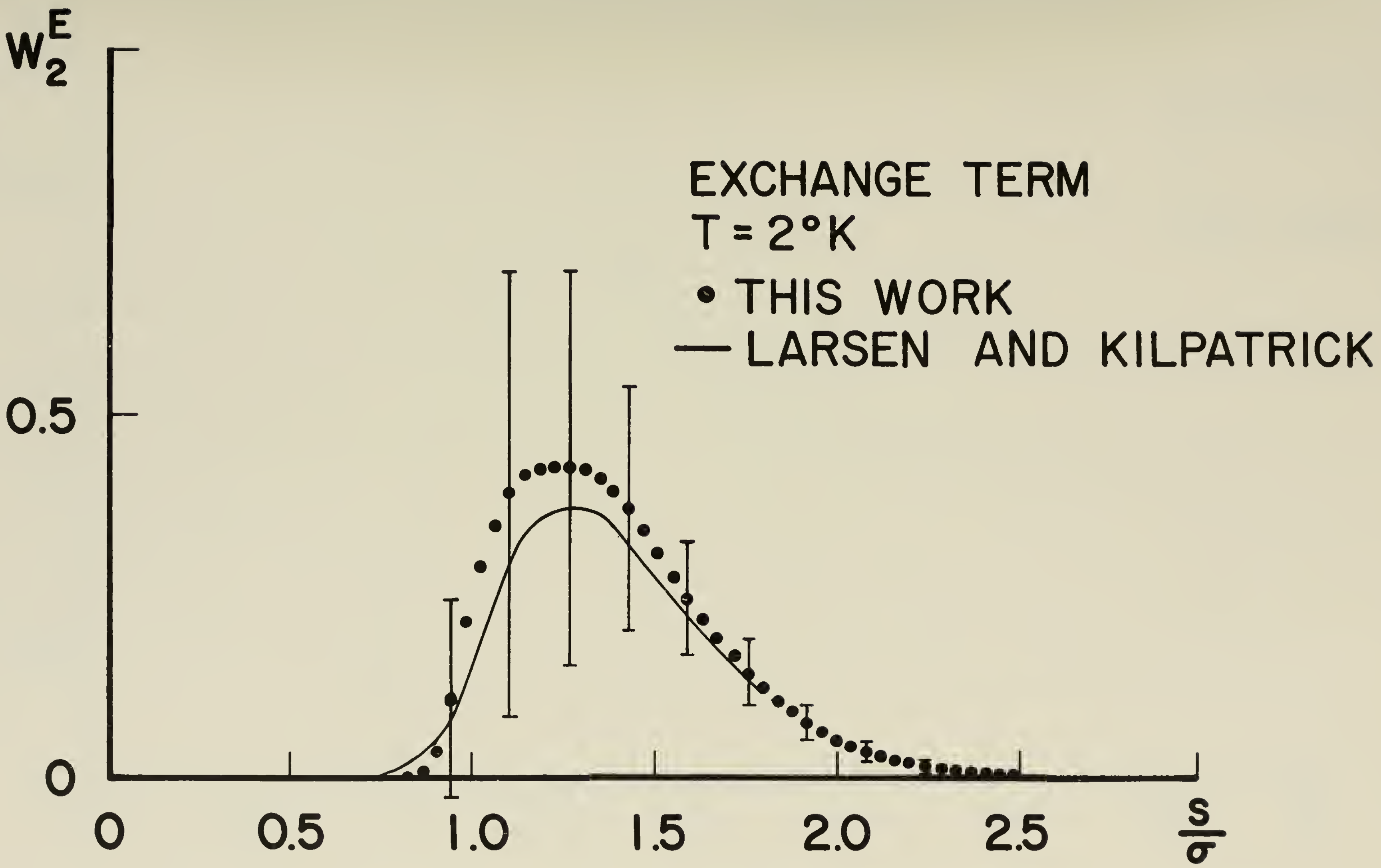
W_2^E
0.5
0
0
0.5
1.0
1.5
2.0
2.5
$\frac{s}{\sigma}$
EXCHANGE TERM
T = 2°K
● THIS WORK
— LARSEN AND KILPATRICK

Figure 7b

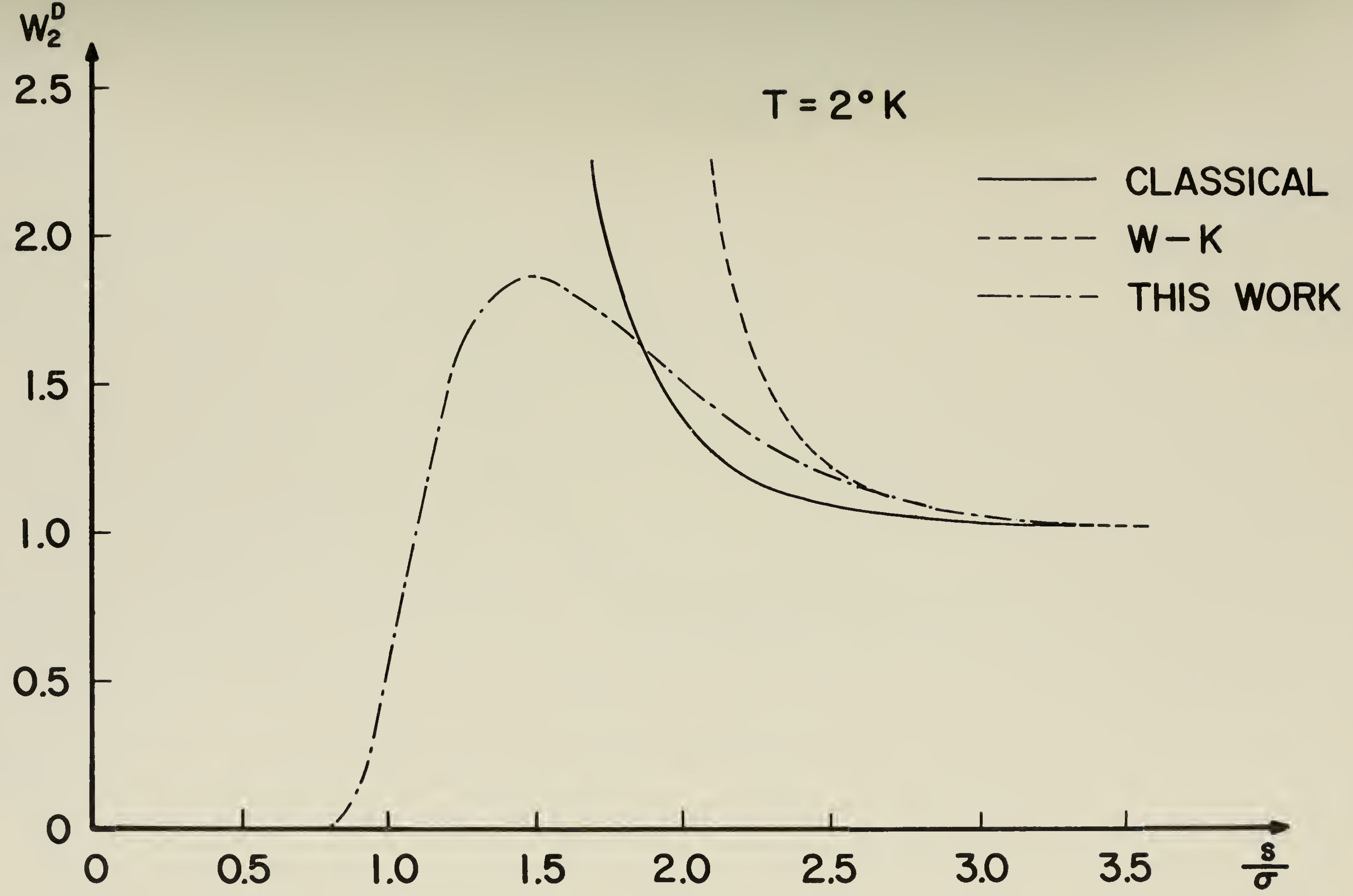
W_2^D
2.5
2.0
1.5
1.0
0.5
0
0
0.5
1.0
1.5
2.0
2.5
3.0
3.5
$\frac{s}{\sigma}$
T = 2° K
CLASSICAL
W – K
THIS WORK

Figure 8a

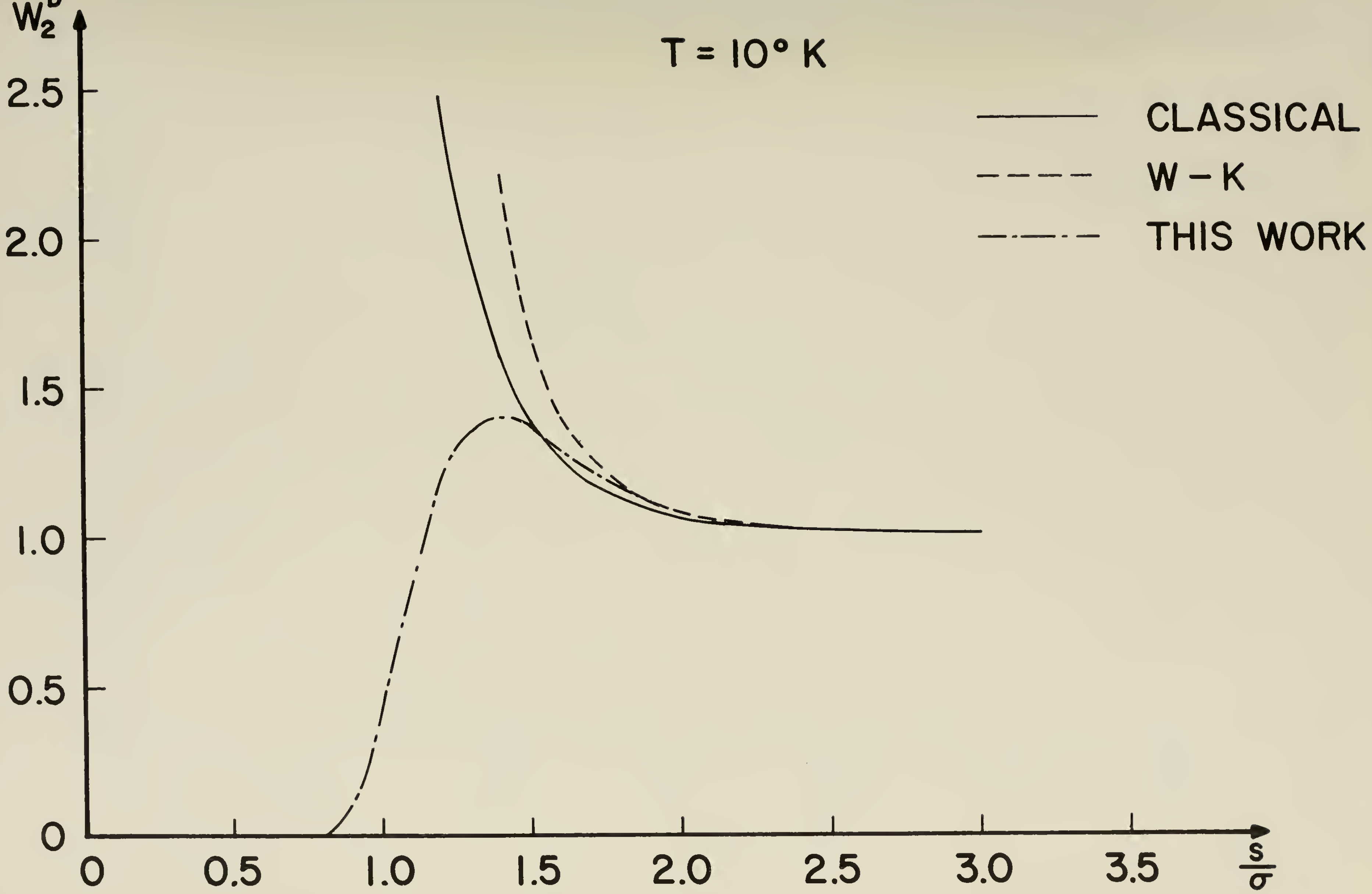
W_2^D
T = 10° K
CLASSICAL
W – K
THIS WORK
2.5
2.0
1.5
1.0
0.5
0
0
0.5
1.0
1.5
2.0
2.5
3.0
3.5
$\frac{s}{\sigma}$

Figure 8b

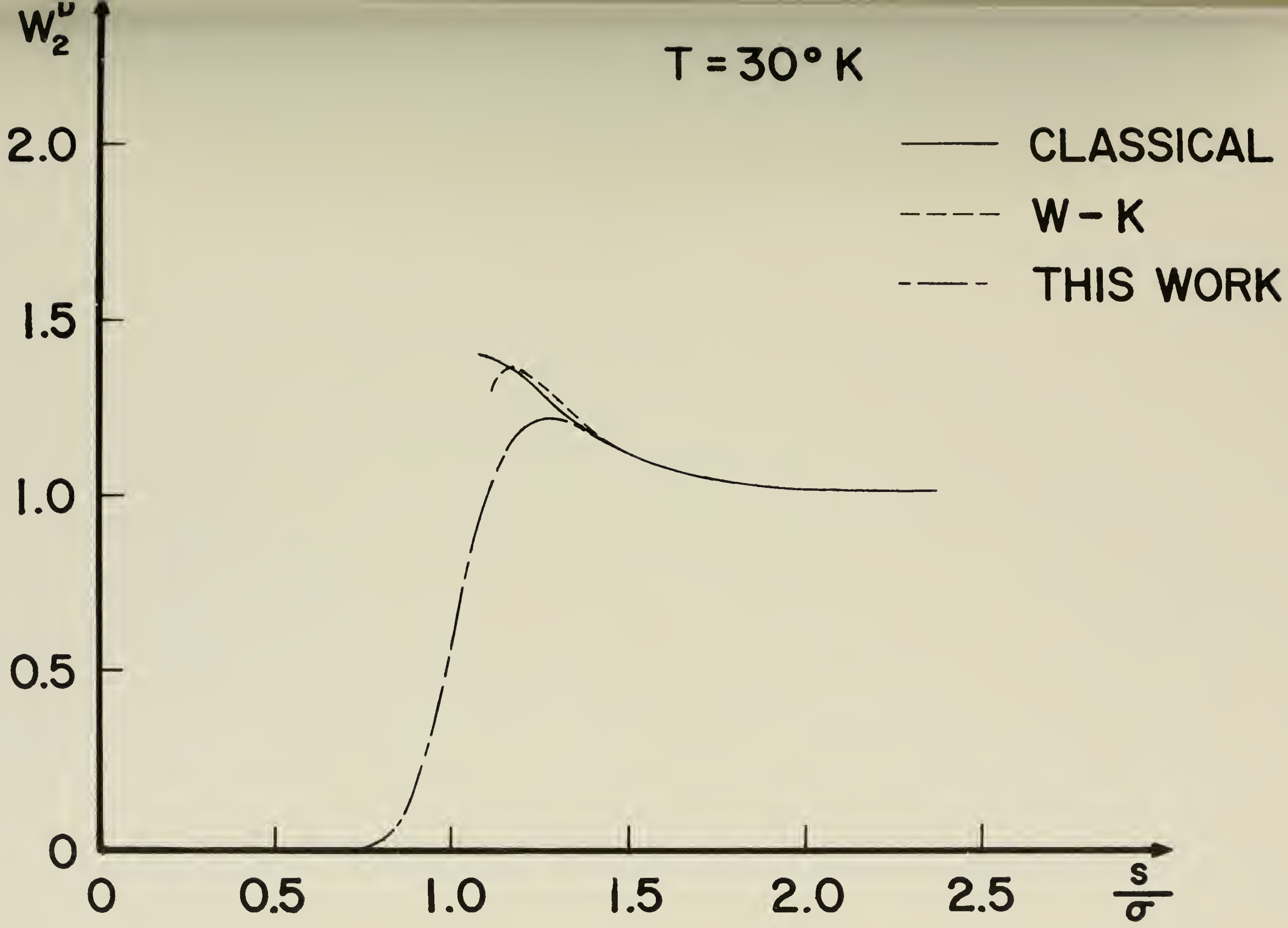
W_2^D
T = 30° K
CLASSICAL
W - K
THIS WORK
2.0
1.5
1.0
0.5
0
0
0.5
1.0
1.5
2.0
2.5
$\frac{s}{\sigma}$

Figure 8c

BOUND BY
HNM

UNIVERSITY OF ILLINOIS-URBANA
510.84 IL6R no. C002 v.171-187(1965)
Illiac III: a processor of visual inform
3 0112 088398208